ACS APPLIED MATERIALS & INTERFACES

Research Article

Cite This: ACS Appl. Mater. Interfaces XXXX, XXX, XXX−XXX

www.acsami.org

Light or Thermally Powered Autonomous Rolling of an Elastomer Rod

Chihyung Ahn,[†,#] Kai Li,[†,§,#] and Shengqiang Cai*[,†,‡]

[†]Materials Science and Engineering Program, University of California, San Diego, La Jolla, California 92093, United States

[‡]Department of Mechanical and Aerospace Engineering, University of California, San Diego, La Jolla, California 92093, United States

[§]Department of Civil Engineering, Anhui Jianzhu University, Hefei, Anhui 230601, China

Supporting Information

ABSTRACT: Specially arranged external stimuli or carefully designed geometry are often essential for realizing continuous autonomous motion of active structures without self-carried power. As a consequence, it is usually very challenging to further integrate those structures as active building blocks into a system with a complex form and multiple functions. In this letter, we report an autonomous motion of a surprisingly simple setup: a cylindrical elastomer rod on a flat hot surface or under homogeneous illumination of visible light. We further show that the rod can roll continuously without any sign of a pause after 6 h, if an obstacle is put in front of it. We demonstrate that such nonintuitive autonomous rolling results from a combination of large thermal actuation of the elastomer and heat transfer between the rod and its surroundings. Quantitative predictions of the rolling speed from the developed thermomechanics model agree reasonably well with experimental measurements. Using the autonomous rolling rods as main building blocks, we further design and fabricate a light-powered vehicle and a thermally powered conveyor for mass transport in both air and water environments.

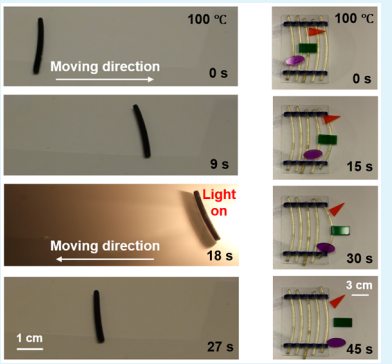

KEYWORDS: *autonomous rolling, liquid crystal elastomer, light-powered motion, thermally powered motion, soft robot*

INTRODUCTION

Controlled movement of tetherless structures, driven by different external stimuli such as light, humidity, heat, and magnetic field, have been recently extensively explored,[1−10] thanks to their potential applications in robotics, biomimetic systems, and energy harvesting devices. To maintain continuous motion of those structures, it is usually required to either introduce spatially heterogeneous stimuli[11] or dynamically control the external stimuli.[12,13] For example, a photosensitive polymeric thin film can swim away from a light source on the surface of water, when the light is periodically turned on and off.[14,15] A hygrobot fabricated from a humidity-sensitive polymer can move along the gradient of environmental humidity.[16] A self-walking gel robot can walk automatically, driven by internal self-oscillating reactions.[17]

Recently, novel structures and devices have been fabricated, which can move ceaselessly under the action of static stimuli.[8,18−21] Autonomous movement of most of those structures relies on carefully designed geometries,[7,24,25] customized material,[1,8,23] and/or specially arranged external stimuli.[3,22] For example, in most light-driven autonomous moving structures, the light has to be illuminated from a certain direction to the active structure.[8,13,23] Although unusual capabilities and intriguing performance of those structures have been demonstrated, it is very challenging to assemble those delicate structures as active building blocks to a system with complex forms and multifunction.

In this article, we report autonomous rolling of a cylindrical monodomain liquid crystal elastomer (LCE) rod on a flat plate with homogeneously elevated temperature or under homogeneous light illumination. Due to the large and reversible actuation strain, high stretchability and excellent programmability, LCE has been recently developed into diverse structures to realize various deformation and motion, triggered by thermal,[24−28] optical,[3,29−35] and magnetic stimuli.[36,37] Different from all the previous studies, continuous and autonomous rolling of an LCE rod observed in the current study does not rely on any complex geometrical design, special patterning of mesogenic molecules, and inhomogeneous or dynamic external stimuli. Autonomous rolling in the current work means that no dynamic control of stimuli is involved, which is also often categorized as self-regulating motion.[10] Based on our understanding of the autonomous rolling mechanism of the LCE rod, we can realize controlled rod rolling through a combination of thermal and optical stimuli. Using autonomous rolling rods as the main building blocks, we further design and fabricate a light-

Received: May 8, 2018
Accepted: July 10, 2018
Published: July 10, 2018

DOI: 10.1021/acsami.8b07563
ACS Appl. Mater. Interfaces XXXX, XXX, XXX−XXX

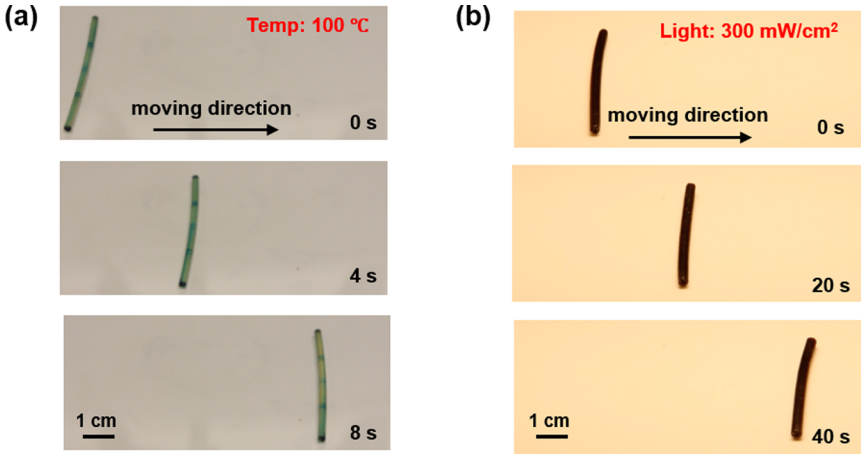

Figure 1. Autonomous rolling of an LCE rod on a plate with homogeneously elevated temperature or under homogeneous light illumination. (a) A cylindrical LCE rod rolls autonomously on a hot plate with homogeneous temperature around 100 °C. (b) A cylindrical LCE-CNT composite rod rolls autonomously under homogeneous illumination of white light with power density of 300 mW/cm^2.

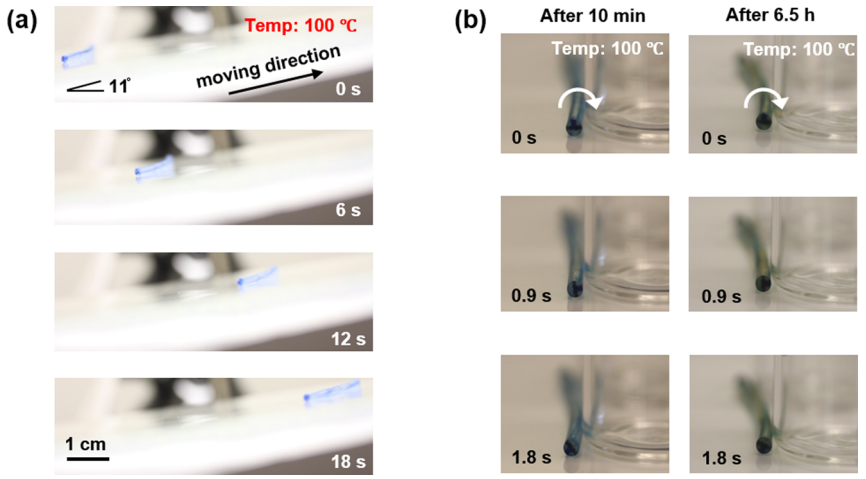

Figure 2. (a) Autonomous climbing LCE rod on a tilted hot surface. (b) Spinning of the same LCE rod blocked by a glass bottle on a hot surface with temperature of 100 °C. Ten minutes after the start of the spinning of the LCE rod, its spinning angular velocity of the rod is around 2.05 rad/s. After 6.5 h, the spinning angular velocity of the rod decreases to 1.75 rad/s.

powered, weight-carrying vehicle and thermally powered conveyor for mass transport in both air and water.

RESULTS AND DISCUSSION

We find in the experiment that a cylindrical (monodomain) LCE rod with 70.0 mm length and 2.6 mm diameter rolls to one direction immediately after it is placed on the top of a flat hot surface with homogeneous temperature around 100 °C. Its rolling speed is around 6 mm/s as shown in Figure 1a (and Movie S1 of the Supporting Information). Inspired by the thermally induced rolling, we further show that similar autonomous rolling can also be powered by homogeneous light illumination for an LCE-carbon nanotube (CNT) composite rod as shown in Figure 1b (and Movie S2 of the Supporting Information). In the experiment, we shed a white light (Hubbell QLI500, halogen lamp) from the top onto the LCE-CNT composite rod with the same size as the pristine LCE rod, which is laid on a flat surface at room temperature. The rod begins to roll to one direction at the speed around 0.3 mm/s, immediately after the light exposure as shown in Movie S2 of the Supporting Information. During the rolling of the elastomer rod as illustrated in Figure 1a and b (and Movies S1 and S2 of the Supporting Information), no sliding between the rod and the surface is observed.

The LCE rod can even roll up on a hot surface with a tilting angle around 11° as shown in Figure 2a (and Movie S3 of the Supporting Information). In this case, the rolling speed of the rod decreases to 3 mm/s, compared to 6 mm/s on a flat surface. With a blockage in front of the LCE rod, it can continuously spin with no sign of stopping after 6 h, though its angular velocity slightly decreases from 2.05 to 1.75 rad/s as shown in Figure 2b (and Movies S4 and S5 of the Supporting Information).

According to our knowledge, the autonomous rolling of an elastomer rod for such a simple setup as described above has never been reported before. We next provide a qualitative interpretation for the phenomenon and later develop a quantitative thermomechanical model for it.

In terms of molecular structure, LCE can be regarded as an integration of mesogenic molecules into a polymer network (Figure S1 of the Supporting Information). Large contraction along the aligning direction of the mesogens can be realized in a monodomain LCE upon heating, caused by the increased disorder of aligned mesogens with temperature increase. Reversible thermal actuation of a monodomain LCE film used

DOI: 10.1021/acsami.8b07563
ACS Appl. Mater. Interfaces XXXX, XXX, XXX−XXX

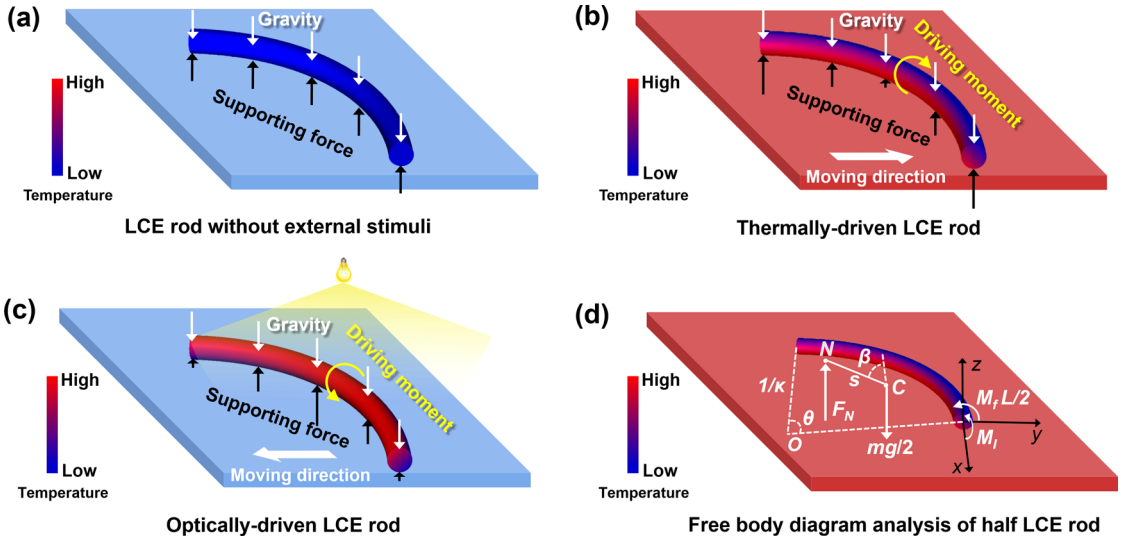

Figure 3. Schematic illustration of the mechanism of autonomous rolling of an LCE rod on a hot surface or under homogeneous light illumination. (a) Initially, for an LCE rod lying on a surface at room temperature, its gravity distributes homogeneously along its length, which is balanced by the supporting force provided by the surface. (b) When the temperature of the surface is elevated, an inhomogeneous temperature field in the LCE rod results in inhomogeneous actuating strain, which tends to bend the middle part of the rod up, and the supporting force gets highly concentrated on the two ends of the rod. Finally, the gravitational force and the supporting force generate a moment driving the LCE rod roll to the direction which it is convex toward. (c) With a light irradiation from the top, the LCE-CNT composite rod has the tendency of bending its two ends up due to the photothermal effect of CNTs which generate thermal gradient along the thickness of the rod. As a result, the supporting force provided by the surface gets concentrated to the middle part of the rod, and the moment generated by the supporting force and gravity drives the rod rolls to its concave direction. (d) Free body diagram analysis of half of the rod, which steadily rolls on a hot plate.

in the current work is shown in Figure S2 of the Supporting Information. For an LCE-CNT composite, similar contraction can be achieved by light illumination due to photothermal effects, as shown in many previous studies.[38−41] We believe the light or thermally powered autonomous rolling of the LCE rod described above are due to the combination of large thermal actuation of LCE material and heat transfer between the elastomer and ambient environment. In the following, we discuss how the LCE rod starts to roll as well as maintains the continuous and steady rolling.

Because the external stimuli, namely the high temperature and light irradiation, are nearly homogeneous in the lateral direction, breaking the geometrical symmetry of a cylindrical rod is necessary for initiating its rolling. In our experiments, we believe it is the initial curvature of the rod (introduced during its fabrication) that breaks the symmetry. Through careful examinations, we find that the degree of curvature of an as-prepared LCE rod as shown in Figure S3a of the Supporting Information, can be as large as 10°, if no special attention is paid during the fabrication. In the autonomous rolling experiments, if we rotate the LCE rod by 180° with respect to its longitudinal axis, the rod rolls to the opposite direction under the same experimental condition, which also indicates the geometric asymmetry of the rod. Moreover, to directly validate the above explanations, we also fabricate LCE rods extremely carefully to significantly reduce their initial bending as shown in Figure S3b of the Supporting Information. We find that those much straighter LCE rods cannot roll spontaneously when they are put onto the same hot surface as shown in the Movie S6 of the Supporting Information.

The moment which drives the LCE rod to roll can be understood in the following force/moment analysis: when a cylindrical LCE rod is placed on a flat plate at room temperature, its gravity is distributed homogeneously along its length. Likewise, the distribution of the supporting force provided by the plate is also homogeneous. Therefore, the supporting force and gravity are balanced with each other as illustrated in Figure 3a. When the temperature of the plate is raised to above the phase transition temperature of the mesogens in the LCE, the bottom of the LCE rod directly in contact with the plate is heated up to a higher temperature than the top of the rod as shown in Figure 3b. Because the contraction of the LCE increases with the increase of temperature, the bottom of the LCE rod tends to contract more along the axial direction than its top part, resulting in an internal bending moment which tends to bend up the middle segment of the rod. As a consequence, the homogeneously distributed supporting force provided by the plate gets more and more concentrated toward the two ends of the rod. In an extreme case, if the LCE rod is clamped by its two ends as shown in Figure S4a of the Supporting Information, due to the bending deformation of the LCE rod, the supporting force finally becomes two point-forces applied onto the two ends. Because of the redistribution of the supporting force and the curved shape of the rod, the gravitational force of the rod and the supporting force provided by the plate can form a couple which drives the rod to roll to the direction which it is convex to, as shown in Figure 3b. After the rolling of the LCE rod is started, the rolling can be maintained because the side of the rod opposite to the rolling direction is always hotter than the other side (Figure 3b), which automatically maintains the lateral bending of the rod. For those straight LCE rods prepared much more carefully as mentioned previously, which cannot spontaneously roll on the hot plate, they can maintain the rolling without requiring any external force or torque, once the rolling is triggered as shown in Movie S6 of the Supporting Information. Therefore, the initial bending of an LCE rod is not critical for the maintenance of the continuous rolling.

Based on the mechanism proposed above, we can easily understand the light-powered rolling of the LCE-CNT composite rod. With a light radiation from the top, the top

DOI: 10.1021/acsami.8b07563
ACS Appl. Mater. Interfaces XXXX, XXX, XXX−XXX

surface of the rod is heated up and tends to contract due to the photothermal effect. As a result, the two ends of the LCE rod has the tendency of bending up, causing the supporting force being concentrated on the middle of the rod. Light-induced bending deformation of an LCE-CNT composite rod is shown in Figure S4b of the Supporting Information. The concentrated supporting force and gravity of the rod can also form a couple which drives the rod to roll to its concave direction as shown in Figure 3c, which is opposite to the thermally powered rolling as discussed above. Such prediction completely agrees with experimental observations (see Movie S6 of the Supporting Information).

According to the understandings of the autonomous rolling mechanism of the elastomer rod, rolling direction of the rod is determined by the direction of its curvature. We next use a light source to induce the reversal of the rolling direction of an LCE-CNT composite rod on a hot plate. In the experiment, an LCE-CNT composite rod first rolls on a hot plate with homogeneous temperature of 100 °C. At a moment, we turn on a light remotely, which makes the rod slow down, stop, and roll to the opposite direction as shown in Figure 4 (Movie S7, Supporting Information). Such light-induced reversal of rod rolling can be easily understood based on the mechanism proposed above. As explained previously, before the light is turned on, the rod rolls on a hot surface to its convex direction. When a light is irradiated onto the LCE rod from its moving direction, the side of the rod facing to the light can absorb light, convert it to heat and tend to contract. As a consequence, the curvature of the rod, and thus its rolling direction, are both reversed to the opposite direction as shown in Figure 4 and Movie S7 of the Supporting Information. Although only light-induced reversal of the rolling is demonstrated in the current work, it is reasonable to expect that by applying inhomogeneous light irradiation onto the LCE-CNT composite rod, we can realize many different rolling paths of the rod on a hot surface, which will be investigated in a follow-up work.

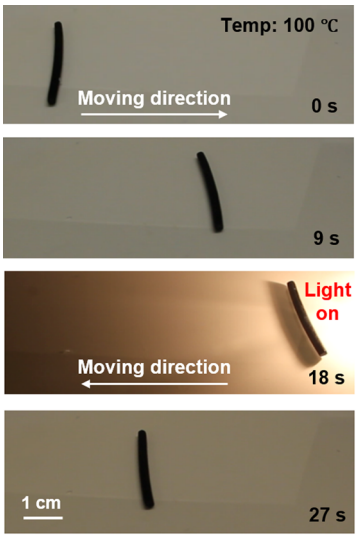

Figure 4. Light-induced reverse rolling of an LCE-CNT composite rod on a flat hot surface. An LCE-CNT composite rod rolls autonomously to its convex direction on a flat hot surface. When we turn on a light, the middle of the rod bends opposite to its rolling direction, and consequently, the rolling of the rod slows down, stops, and then reverses. The rod moves to the opposite direction steadily after the light is turned off.

Based on the above qualitative understanding, we next develop a quantitative thermomechanical model for steady autonomous rolling of an LCE rod on a flat hot surface. We select half of the rod to conduct free body diagram analysis as shown in Figure 3d. During the steady rolling, the LCE rod is curved laterally on the surface as observed in the experiments and explained previously. The radius of curvature of the rod in the plane is denoted by κ. In the free body diagram analysis, we regard the gravitational force of the half rod (with length L) as a single force acting on its gravity center as shown in Figure 3d. Likewise, we also regard the distributed supporting force as single force acting on another point. Without losing generality, the acting point of the supporting force is assumed to be different from the gravity center of the half rod, and the distance between the two points is assumed to be s. Because of the temperature gradient in the rod, thermal contraction of the rod along the axial direction is not homogeneous, resulting in an internal bending moment, denoted by M_I in y direction as shown in Figure 3d. During the steady rolling, the rolling resistance per length of the rod is denoted by M_f in the x direction. We can obtain the relationship between the internal bending moment and rolling resistance based on simple moment balance analysis (more details can be found in the Supporting Information):

$$M_f = \frac{2}{3}\kappa M_I \tag{1}$$

The rolling resistance per unit length of a cylindrical rod can be empirically given as

$$M_f = C_{rr}R\rho g\pi R^2 \tag{2}$$

where C_{rr} is the rolling frictional coefficient, R is the radius of the rod, and ρ is its mass density.

During the rolling, there is no vertical bending deformation of the rod. Therefore, the magnitude of internal bending moment can be related to the temperature field $T(r, \theta)$ in the cross section of the rod as (the polar coordinate system of the cross section of the rod can be found in the Figure S5 of the Supporting Information):

$$M_I = \int_0^{2\pi}\int_0^R T(r, \theta)\alpha E r \cos\theta r \, \mathrm{d}r \, \mathrm{d}\theta \tag{3}$$

where α is the effective thermal contraction coefficient and E is the elastic modulus of the LCE rod along its axial direction. In eq 3 and below, we assume the relationship between thermal contraction strain and temperature change is linear; we also adopt the linear elasticity assumption.

Similarly, the lateral bending curvature κ resulting from the inhomogeneous temperature field of the rod can be computed as

$$\kappa = \frac{1}{EI}\int_0^{2\pi}\int_0^R T(r, \theta)\alpha E r \sin\theta r \, \mathrm{d}r \, \mathrm{d}\theta \tag{4}$$

where EI is the bending stiffness of the rod.

As shown in eq 1, the internal bending moment in the rod drives the rod to roll. To maintain the steady rolling, the thermal bending moment computed in eq 3 should be comparable to the rolling resistance, which implies that the large thermal actuation of LCE is critical for its autonomous rolling on a surface with large frictional coefficient.

To obtain the internal bending moment M_I and the lateral bending curvature κ, we need to determine the temperature field

DOI: 10.1021/acsami.8b07563
ACS Appl. Mater. Interfaces XXXX, XXX, XXX−XXX

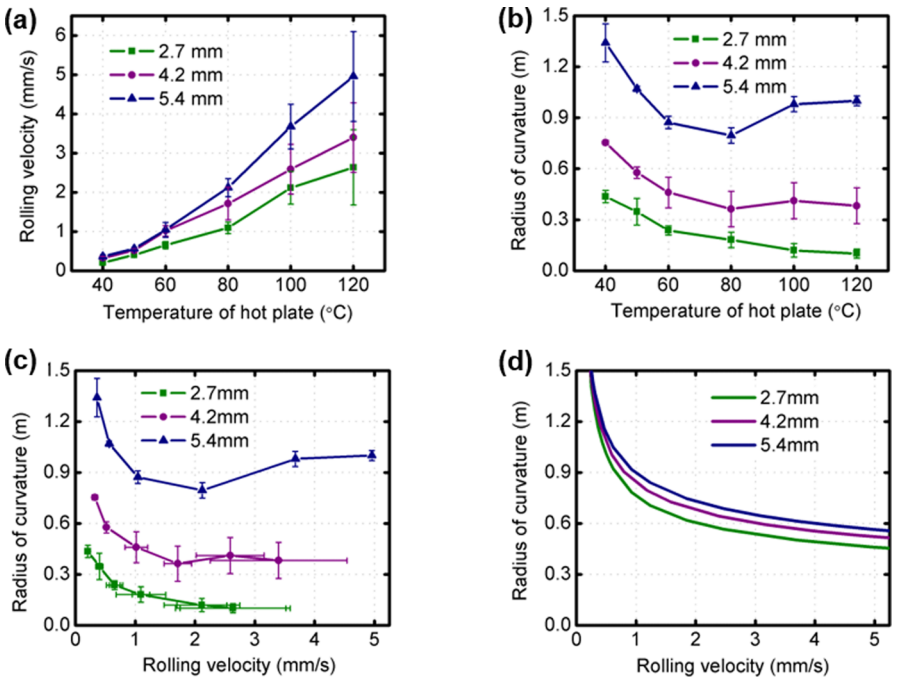

Figure 5. Experimental measurements of (a) rolling velocity and (b) radius of lateral curvature of LCE rods with different diameters on a hot plate at different temperatures. (c) Experimental results and (d) theoretical predictions of the relationship between the radius of lateral curvature and rolling velocity of LCE rods with different diameters. For each data point, experimental measurements are conducted on five LCE rods with same diameter and prepared in the same conditions.

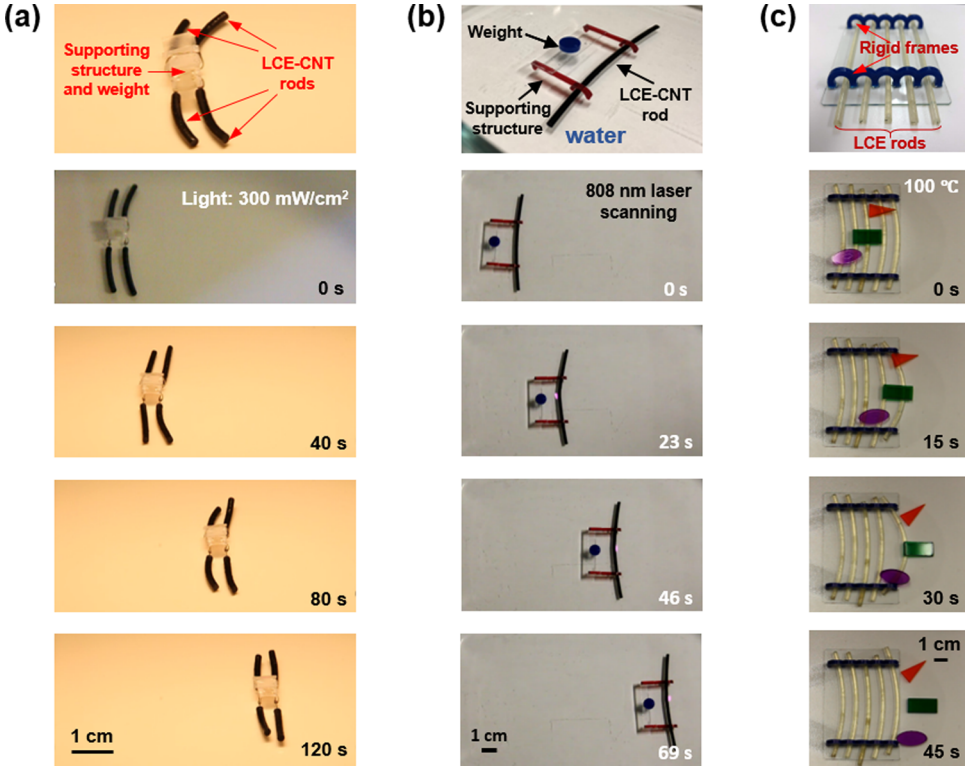

Figure 6. Demonstrations of active structures composed of LCE rods as active building blocks. (a) A vehicle composed of four LCE-CNT rod wheels can move on a flat surface under light illumination. (b) LCE-CNT rod rolls under water induced by laser scanning while carrying weight. (c) Thermally driven LCE conveyor transports weights by its continuous rolling on a hot surface.

in the cross section of the rod. For a steady rolling rod on a hot plate, the temperature field in its cross section can be written in a dimensionless form: $T = \frac{QR}{k} f\left(\bar{r}, \theta; \frac{V}{V_0}, \frac{R}{R_0}\right)$, with $\bar{r} = r/R$, $V_0 = k/\rho cR$, and $R_0 = k/h$, in which Q is heat influx from the hot plate, k is the thermal conductivity of the rod, c is the specific heat of the rod, V is the rolling velocity of the rod, and h is the heat-transfer coefficient between the rod and its surroundings.

DOI: 10.1021/acsami.8b07563
ACS Appl. Mater. Interfaces XXXX, XXX, XXX−XXX

The explicit form of the function $f\left(\bar{r}, \theta; \frac{V}{V_0}, \frac{R}{R_0}\right)$ can be found in the Supporting Information. As shown in Figure S6 of the Supporting Information, the bottom of the rod has higher temperature then the top, and the side facing to the rolling direction is cooler than the other side, which agrees with our previous qualitative interpretation. Finally, a combination of eq 3 and the temperature field gives the internal bending moment as

$$M_I = \frac{\alpha E Q R^4}{k} g_1\left(\frac{V}{V_0}, \frac{R}{R_0}\right) \tag{5}$$

where $g_1\left(\frac{V}{V_0}, \frac{R}{R_0}\right) = \int_0^{2\pi}\int_0^1 f\left(\bar{r}, \theta; \frac{V}{V_0}, \frac{R}{R_0}\right)\bar{r}^2 \cos\theta \, d\bar{r} \, d\theta$. The lateral bending curvature κ can also be given by

$$\kappa = \frac{4\alpha Q}{\pi k} g_2\left(\frac{V}{V_0}, \frac{R}{R_0}\right) \tag{6}$$

where $g_2 = \int_0^{2\pi}\int_0^1 f\left(\bar{r}, \theta; \frac{V}{V_0}, \frac{R}{R_0}\right)\bar{r}^2 \sin\theta \, d\bar{r} \, d\theta$.

Although the heat influx Q is challenging to determine for the current thermal contact problem, we obtain an explicit relationship between the lateral bending curvature and the rolling velocity based on eq 1, 2, 5, and 6:

$$\kappa^2 = \frac{6C_{rr}\rho g}{ER} \frac{g_2\left(\frac{V}{V_0}, \frac{R}{R_0}\right)}{g_1\left(\frac{V}{V_0}, \frac{R}{R_0}\right)} \tag{7}$$

To validate our theory developed above, we further conduct systematic experiments on the rolling of LCE rods with three different diameters on a hot surface at different temperatures. The lateral bending curvature κ and rolling speed V of the LCE rods with three different diameters are plotted as functions of the temperature in Figures 5a and b, respectively. In addition, based on Figures 5a and b, we further plot the relationship between the lateral bending curvature κ and rolling speed V of the LCE rods for different diameters as shown in Figure 5c. The predictions from eq 7 with one set of material parameters as summarized in Table S1 of the Supporting Information are plotted in Figure 5d. It is noted that all the material parameters are assumed to be independent of the size of the LCE rod and temperature, which is a rough approximation. With considering all the simplifications, we think the agreement between the theory and experimental measurements is satisfactory. It will be more complex to quantitatively predict the rolling of LCE-CNT composite rods under light illumination, which is beyond the scope of the article.

Due to the simplicity of the autonomous rolling of an LCE rod discovered by us, we next assemble the LCE rods to three different functional devices which can be powered by heat or light, respectively. The first device is a light-powered weight-carrying vehicle as shown in Figure 6a and Movie S8. The vehicle is simply composed of four LCE-CNT composite rods as active wheels connected to a wire as supporting structure. Rolling of the four wheels can finally result in translational motion of the vehicle. In the experiment as shown in Figure 6a, we put a weight of roughly two times of the weight of the LCE rods on a supporting structure. Under the illumination of white light, the LCE vehicle can move forward with a speed around 0.2 mm/s.

To demonstrate the robustness of the autonomous rolling, we further show that a similar light-powered LCE vehicle can move underwater (see Figure 6b and Movie S9 of the Supporting Information). In the design, a single LCE-CNT composite rod is used as the driving wheel for the vehicle. With a continuous nIR-laser scanning along the axial direction of the rod from the top, the vehicle can move under water with a speed around 2.0 mm/s while carrying a small weight.

The third device is a thermally powered LCE conveyor as shown in Figure 6c and Movie S10 of the Supporting Information. Five LCE rods are placed parallel on the top of a hot surface. To prevent translational motion, both ends of each rod are constrained by small holes of rigid frames, which are glued onto the substrate. Blocks of different shapes can be transported on the conveyor from one side to the other side with the speed around 1.7 mm/s. Each block has a weight comparable to that of an LCE rod.

The three functional devices shown in Figure 6 clearly demonstrate the potential applications of the light or thermally driven autonomous rolling of LCE rods discovered in the current study. Due to the simple geometry and high robustness of the rolling mechanism, advanced active structures of more complex forms and with multiple functionalities can also be constructed based on various combinations of LCE rods.

CONCLUSION

In this article, we report a discovery of autonomous rolling phenomenon in a surprisingly simple setup: a cylindrical elastomer rod on a flat hot surface with homogeneous temperature or under homogeneous illumination of light. We find that a combination of thermally driven active deformation of the elastomer and heat transfer between the rod and its surrounding is the key for the autonomous rolling of the rod. To obtain more quantitative understanding, we develop a thermomechanical model for the autonomous rolling phenomenon. Based on our understanding, we successfully use a white light source to induce the reversal of thermally powered rod rolling. In addition, using the autonomous rolling rods as the active building blocks, we design and fabricate a light-powered weight-carrying vehicle and a thermally powered conveyor.

EXPERIMENTAL METHODS

Materials. LC monomer, 1,4-bis-[4-(3-acryloyloxypropyloxy)-benzoyloxy]-2-methylbenzene (95%, RM257), is purchased from Wilshire Technologies. Cross-linker, pentaerythritol tetrakis(3-mercaptopropionate) (95%, PETMP), spacer, 2,2′-(ethylenedioxy) diethanethiol (95%, EDDET), catalyst, dipropyl amine (98%, DPA), photoinitiator, (2-hydroxyethoxy)-2-methylpropiophenone (98%, HHMP), and multiwalled carbon nanotubes (98%, CNTs) are purchased from Aldrich. All chemicals are used as received without any purification.

Fabrication of LCE Rods. LCE rods are prepared by the two-step cross-linking reaction according to the method previously reported by Yakacki et al.[42] The LCE monomer mixture is prepared by dissolving RM257 (LC monomer), PETMP (cross-linker), EDDET (spacer), and HHMP (photoinitiator) in toluene followed by heating above LC phase transition temperature and vigorous mixing. The composition of the mixture consists of 53.0 wt % of RM257, 2.5 wt % of PETMP, 12.5 wt % of EDDET, and 0.4 wt % of HHMP in toluene. After the mixture becomes homogeneous, 0.2 wt % of DPA (catalyst) is added to trigger the reaction. For LCE-CNT composite, 0.2 wt % of CNTs are also added in the mixture. The mixture is placed in the vacuum chamber to remove bubbles trapped inside, followed by being transferred into a cylindrical mold as shown in Figure S1 of the Supporting Information. The mixture is left overnight at room temperature to be loosely cross-

DOI: 10.1021/acsami.8b07563
ACS Appl. Mater. Interfaces XXXX, XXX, XXX−XXX

linked by the thiol−acrylate Michael addition reaction. The loosely cross-linked LCE rod is placed in the oven at 80 °C for 24 h for the evaporation of residual solvent. After the LCE rod is dried, it is subjected to uniaxial stretch to achieve monodomain state[15,42] and under the UV light (365 nm, UVP B-100AP/R) irradiation for 1 h to be fully cross-linked. Finally, the LCE rod in a cylindrical shape with different diameters can be obtained.

Heat and Light-Induced Rolling. The temperature of the hot plate (Corning PC-420D) is set up as a desired temperature and then LCE rod is placed on the top of it to initiate heat-induced rolling motion. For the light-induced rolling, LCE-CNT rod is placed below a white light source (Hubbell QLI500, halogen lamp) with distance about 20 cm. The LCE-CNT rod begins to move once the light is turned on.

Light-Induced Rolling Reversal. The rolling direction of the LCE rod can be reversed by irradiation of visible light (Hubbell QLI500, halogen lamp) on the convex surface of the LCE rod. The light is turned on 20 cm away from the LCE rod while it is rolling. Once the rolling direction of the LCE rod is reversed, no further light irradiation is required.

Fabrication of LCE Rod-Based Active Structures. Two pairs of LCE-CNT rods, as wheels of the light-powered LCE vehicle, are connected by aluminum wires with diameter of 0.3 mm. A supporting frame structure is built on the connecting wires. For the weight-carrying LCE-CNT rod under water, an LCE-CNT rod is placed under water and two laser-cut acrylic structures connected by a transparent acrylic sheet are placed on top of it. The LCE-CNT rod rolls and drags the structure forward under water, when a laser is scanned along the length of the rod. The thermally driven LCE conveyor is made by placing five LCE rods in parallel on the top of a hot surface. Two acrylic structures with five holes are placed at each end of the LCE rods to prevent the translation.

■ ASSOCIATED CONTENT

Supporting Information

The Supporting Information is available free of charge on the ACS Publications website at DOI: 10.1021/acsami.8b07563.

More details for the theoretical predictions, schematic of experimental procedure, photos of the LCE rod's initial curvature and deformation, cross-sectional schematic of rolling rod, temperature field analysis of rolling rod, and stress−strain diagram of LCE film (PDF)

Movie S1: Autonomous rolling of an LCE rod on a hot surface with homogeneous temperature (AVI)

Movie S2: Autonomous rolling of an LCE-CNT composite rod on a surface under homogeneous light illumination (AVI)

Movie S3: Autonomous climbing of an LCE rod on a tilted hot surface (AVI)

Movie S4: Spinning of an LCE rod on a hot surface in front of a blockage (10 mins after the start of the spinning) (AVI)

Movie S5: Spinning of an LCE rod on a hot surface in front of a blockage (6.5 h after the start of the spinning) (AVI)

Movie S6: A straight LCE rod cannot roll automatically on a hot surface, but it can maintain continuous rolling after it is pushed by an external force (AVI)

Movie S7: Light-induced reverse rolling of an LCE-CNT composite rod on a flat hot surface (AVI)

Movie S8: A light-powered vehicle with LCE-CNT composite rods as wheels (AVI)

Movie S9: A laser-powered vehicle with LCE-CNT composite rod moving under water (AVI)

Movie S10: A thermally powered LCE rod conveyor (AVI)

■ AUTHOR INFORMATION

Corresponding Author

*E-mail: shqcai@ucsd.edu (S.C.).

ORCID

Shengqiang Cai: 0000-0002-6852-7680

Author Contributions

#C.A. and K.L. contributed equally to this work.

Notes

The authors declare no competing financial interest.

■ ACKNOWLEDGMENTS

S.C. acknowledges the support from the National Science Foundation through Grant No. CMMI-1554212 and ONR through Grant No. N00014-17-1-2056. K.L. acknowledges the support from the Chinese Natural Science Foundation (Grant No. 11402001).

■ REFERENCES

(1) Hu, W.; Lum, G. Z.; Mastrangeli, M.; Sitti, M. Small-Scale Soft-Bodied Robot with Multimodal Locomotion. *Nature* **2018**, *554*, 81−85.

(2) Zhang, L.; Qiu, X.; Yuan, Y.; Zhang, T. Humidity- and Sunlight-driven Motion of a Chemically Bonded Polymer Bilayer with Programmable Surface Patterns. *ACS Appl. Mater. Interfaces* **2017**, *9*, 41599−41606.

(3) Zeng, H.; Wani, O. M.; Wasylczyk, P.; Priimagi, A. Light-Driven, Caterpillar-Inspired Miniature Inching Robot. *Macromol. Rapid Commun.* **2018**, *39*, 1700224.

(4) Dai, B.; Wang, J.; Xiong, Z.; Zhan, X.; Dai, W.; Li, C.-C.; Feng, S.-P.; Tang, J. Programmable Artificial Phototactic Microswimmer. *Nat. Nanotechnol.* **2016**, *11*, 1087−1093.

(5) Wang, E.; Desai, M. S.; Lee, S.-W. Light-Controlled Graphene-Elastin Composite Hydrogel Actuators. *Nano Lett.* **2013**, *13*, 2826−2830.

(6) Hu, Y.; Liu, J.; Chang, L.; Yang, L.; Xu, A.; Qi, K.; Lu, P.; Wu, G.; Chen, W.; Wu, Y. Electrically and Sunlight-Driven Actuator with Versatile Biomimetic Motions Based on Rolled Carbon Nanotube Bilayer Composite. *Adv. Funct. Mater.* **2017**, *27*, 1704388.

(7) Wie, J. J.; Shankar, M. R.; White, T. J. Photomotility of Polymers. *Nat. Commun.* **2016**, *7*, 13260.

(8) Zhang, X.; Yu, Z.; Wang, C.; Zarrouk, D.; Seo, J.-W. T.; Cheng, J. C.; Buchan, A. D.; Takei, K.; Zhao, Y.; Ager, J. W.; Zhang, J.; Hettick, M.; Hersam, M. C.; Pisano, A. P.; Fearing, R. S.; Javey, A. Photoactuators and Motors Based on Carbon Nanotubes with Selective Chirality Distributions. *Nat. Commun.* **2014**, *5*, 2983.

(9) Gelebart, A. H.; Jan Mulder, D.; Varga, M.; Konya, A.; Vantomme, G.; Meijer, E. W.; Selinger, R. L. B.; Broer, D. J. Making Waves in a Photoactive Polymer Film. *Nature* **2017**, *546*, 632−636.

(10) Zeng, H.; Wasylczyk, P.; Wiersma, D. S.; Priimagi, A. Light Robots: Bridging the Gap between Microrobotics and Photomechanics in Soft Materials. *Adv. Mater.* **2018**, *30*, 1703554.

(11) Palagi, S.; Mark, A. G.; Reigh, S. Y.; Melde, K.; Qiu, T.; Zeng, H.; Parmeggiani, C.; Martella, D.; Sanchez-Castillo, A.; Kapernaum, N.; Giesselmann, F.; Wiersma, D. S.; Lauga, E.; Fischer, P. Structured Light Enables Biomimetic Swimming and Versatile Locomotion of Photoresponsive Soft Microrobots. *Nat. Mater.* **2016**, *15*, 647−653.

(12) Rogóż, M.; Zeng, H.; Xuan, C.; Wiersma, D. S.; Wasylczyk, P. Light-Driven Soft Robot Mimics Caterpillar Locomotion in Natural Scale. *Adv. Opt. Mater.* **2016**, *4*, 1689−1694.

(13) Jiang, W.; Niu, D.; Liu, H.; Wang, C.; Zhao, T.; Yin, L.; Shi, Y.; Chen, B.; Ding, Y.; Lu, B. Photoresponsive Soft-Robotic Platform: Biomimetic Fabrication and Remote Actuation. *Adv. Funct. Mater.* **2014**, *24*, 7598−7604.

(14) Camacho-Lopez, M.; Finkelmann, H.; Palffy-Muhoray, P.; Shelley, M. Fast Liquid-Crystal Elastomer Swims into the Dark. *Nat. Mater.* **2004**, *3*, 307−310.

DOI: 10.1021/acsami.8b07563
ACS Appl. Mater. Interfaces XXXX, XXX, XXX−XXX

(15) Tian, H.; Wang, Z.; Chen, Y.; Shao, J.; Gao, T.; Cai, S. Polydopamine-Coated Main-Chain Liquid Crystal Elastomer as Optically Driven Artificial Muscle. *ACS Appl. Mater. Interfaces* **2018**, *10*, 8307−8316.
(16) Shin, B.; Ha, J.; Lee, M.; Park, K.; Park, G. H.; Choi, T. H.; Cho, K.-J.; Kim, H.-Y. Hygrobot: A Self-Locomotive Ratcheted Actuator Powered by Environmental Humidity. *Sci. Robot.* **2018**, *3*, 2629.
(17) Maeda, S.; Hara, Y.; Sakai, T.; Yoshida, R.; Hashimoto, S. Self-Walking Gel. *Adv. Mater.* **2007**, *19*, 3480−3484.
(18) Maggi, C.; Saglimbeni, F.; Dipalo, M.; De Angelis, F.; Di Leonardo, R. Micromotors with Asymmetric Shape that Efficiently Convert Light into Work by Thermocapillary Effects. *Nat. Commun.* **2015**, *6*, 7855.
(19) Tang, R.; Liu, Z.; Xu, D.; Liu, J.; Yu, L.; Yu, H. Optical Pendulum Generator Based on Photomechanical Liquid-Crystalline Actuators. *ACS Appl. Mater. Interfaces* **2015**, *7*, 8393−8397.
(20) Yu, L.; Yu, H. Light-Powered Tumbler Movement of Graphene Oxide/Polymer Nanocomposites. *ACS Appl. Mater. Interfaces* **2015**, *7*, 3834−3839.
(21) Zeng, H.; Wasylczyk, P.; Parmeggiani, C.; Martella, D.; Burresi, M.; Wiersma, D. S. Light-Fueled Microscopic Walkers. *Adv. Mater.* **2015**, *27*, 3883−3887.
(22) Yamada, M.; Kondo, M.; Miyasato, R.; Naka, Y.; Mamiya, J.-i.; Kinoshita, M.; Shishido, A.; Yu, Y.; Barrett, C. J.; Ikeda, T. Photomobile Polymer Materials-Various Three-Dimensional Movements. *J. Mater. Chem.* **2009**, *19*, 60−62.
(23) Hu, Y.; Wu, G.; Lan, T.; Zhao, J.; Liu, Y.; Chen, W. A Graphene-Based Bimorph Structure for Design of High Performance Photo-actuators. *Adv. Mater.* **2015**, *27*, 7867−7873.
(24) Ostrom, H.; Oberg, H.; Xin, H.; LaRue, J.; Beye, M.; Dell'Angela, A. M.; Gladh, J.; Ng, M. L.; Sellberg, J. A.; Kaya, S.; Mercurio, G.; Nordlund, D.; Hantschmann, M.; Hieke, F.; Kuhn, D.; Schlotter, W. F.; Dakovski, G. L.; Turner, J. J.; Minitti, M. P.; Mitra, A.; Moeller, S. P.; Fohlisch, A.; Wolf, M.; Wurth, W.; Persson, M.; Norskov, J. K.; Abild-Pedersen, F.; Ogasawara, H.; Pettersson, L. G. M.; Nilsson, A. Voxelated Liquid Crystal Elastomers. *Science* **2015**, *347*, 978−982.
(25) Shahsavan, H.; Salili, S. M.; Jákli, A.; Zhao, B. Smart Muscle-Driven Self-Cleaning of Biomimetic Microstructures from Liquid Crystal Elastomers. *Adv. Mater.* **2015**, *27*, 6828−6833.
(26) Sawa, Y.; Urayama, K.; Takigawa, T.; DeSimone, A.; Teresi, L. Thermally Driven Giant Bending of Liquid Crystal Elastomer Films with Hybrid Alignment. *Macromolecules* **2010**, *43*, 4362−4369.
(27) Agrawal, A.; Luchette, P.; Palffy-Muhoray, P.; Biswal, S. L.; Chapman, W. G.; Verduzco, R. Surface Wrinkling in Liquid Crystal Elastomers. *Soft Matter* **2012**, *8*, 7138−7142.
(28) Ahn, C.; Liang, X.; Cai, S. Inhomogeneous Stretch Induced Patterning of Molecular Orientation in Liquid Crystal Elastomers. *Extreme Mech. Lett.* **2015**, *5*, 30−36.
(29) Zeng, H.; Wani, O. M.; Wasylczyk, P.; Kaczmarek, R.; Priimagi, A. Self-Regulating Iris Based on Light-Actuated Liquid Crystal Elastomer. *Adv. Mater.* **2017**, *29*, 1701814.
(30) Jiang, Z.; Xu, M.; Li, F.; Yu, Y. Red-Light-Controllable Liquid-Crystal Soft Actuators via Low-Power Excited Upconversion Based on Triplet−Triplet Annihilation. *J. Am. Chem. Soc.* **2013**, *135*, 16446−16453.
(31) Liu, W.; Guo, L.-X.; Lin, B.-P.; Zhang, X.-Q.; Sun, Y.; Yang, H. Near-Infrared Responsive Liquid Crystalline Elastomers Containing Photothermal Conjugated Polymers. *Macromolecules* **2016**, *49*, 4023−4030.
(32) Kumar, K.; Knie, C.; Bléger, D.; Peletier, M. A.; Friedrich, H.; Hecht, S.; Broer, D. J.; Debije, M. G.; Schenning, A. P. H. J. A Chaotic Self-Oscillating Sunlight-Driven Polymer Actuator. *Nat. Commun.* **2016**, *7*, 11975.
(33) Ikeda, T.; Nakano, M.; Yu, Y. L.; Tsutsumi, O.; Kanazawa, A. Anisotropic Bending and Unbending behavior of Azobenzene Liquid-Crystalline Gels by Light Exposure. *Adv. Mater.* **2003**, *15*, 201−205.
(34) Lee, K. M.; Koerner, H.; Vaia, R. A.; Bunning, T. J.; White, T. J. Light-Activated Shape Memory of Glassy, Azobenzene Liquid Crystalline Polymer Networks. *Soft Matter* **2011**, *7*, 4318−4324.
(35) van Oosten, C. L.; Bastiaansen, C. W. M.; Broer, D. J. Printed Artificial Cilia from Liquid-Crystal Network Actuators Modularly Driven by Light. *Nat. Mater.* **2009**, *8*, 677−682.
(36) Haberl, J. M.; Sánchez-Ferrer, A.; Mihut, A. M.; Dietsch, H.; Hirt, A. M.; Mezzenga, R. Liquid-Crystalline Elastomer-Nanoparticle Hybrids with Reversible Switch of Magnetic Memory. *Adv. Mater.* **2013**, *25*, 1787−1791.
(37) Song, H. M.; Kim, J. C.; Hong, J. H.; Lee, Y. B.; Choi, J.; Lee, J. I.; Kim, W. S.; Kim, J. H.; Hur, N. H. Magnetic and Transparent Composites by Linking Liquid Crystals to Ferrite Nanoparticles through Covalent Networks. *Adv. Funct. Mater.* **2007**, *17*, 2070−2076.
(38) Li, C.; Liu, Y.; Lo, C.-w.; Jiang, H. Reversible White-Light Actuation of Carbon Nanotube Incorporated Liquid Crystalline Elastomer Nanocomposites. *Soft Matter* **2011**, *7*, 7511−7516.
(39) Li, C.; Liu, Y.; Huang, X.; Jiang, H. Direct Sun-Driven Artificial Heliotropism for Solar Energy Harvesting Based on a Photo-Thermomechanical Liquid-Crystal Elastomer Nanocomposite. *Adv. Funct. Mater.* **2012**, *22*, 5166−5174.
(40) Shi Kam, N. W. S.; O'Connell, M.; Wisdom, J. A.; Dai, H. Carbon Nanotubes as Multifunctional Biological Transporters and Near-Infrared Agents for Selective Cancer Cell Destruction. *Proc. Natl. Acad. Sci. U. S. A.* **2005**, *102*, 11600−11605.
(41) Fujigaya, T.; Morimoto, T.; Nakashima, N. Isolated Single-Walled Carbon Nanotubes in a Gel as a Molecular Reservoir and its Application to Controlled Drug Release Triggered by Near-IR Laser Irradiation. *Soft Matter* **2011**, *7*, 2647−2652.
(42) Yakacki, C. M.; Saed, M.; Nair, D. P.; Gong, T.; Reed, S. M.; Bowman, C. N. Tailorable and Programmable Liquid-Crystalline Elastomers Using a Two-Stage Thiol−Acrylate Reaction. *RSC Adv.* **2015**, *5*, 18997−19001.

DOI: 10.1021/acsami.8b07563
ACS Appl. Mater. Interfaces XXXX, XXX, XXX−XXX